nature ecology & evolution

ARTICLES

https://doi.org/10.1038/s41559-022-01668-4

Check for updates

An earlier start of the thermal growing season enhances tree growth in cold humid areas but not in dry areas

Shan Gao[1], Eryuan Liang[1]✉, Ruishun Liu[1], Flurin Babst[2,3], J. Julio Camarero[4], Yongshuo H. Fu[5], Shilong Piao[1,6], Sergio Rossi[7,8], Miaogen Shen[9], Tao Wang[1] and Josep Peñuelas[10,11]

Climatic warming alters the onset, duration and cessation of the vegetative season. While previous studies have shown a tight link between thermal conditions and leaf phenology, less is known about the impacts of phenological changes on tree growth. Here, we assessed the relationships between the start of the thermal growing season and tree growth across the extratropical Northern Hemisphere using 3,451 tree-ring chronologies and daily climatic data for 1948–2014. An earlier start of the thermal growing season promoted growth in regions with high ratios of precipitation to temperature but limited growth in cold–dry regions. Path analyses indicated that an earlier start of the thermal growing season enhanced growth primarily by alleviating thermal limitations on wood formation in boreal forests and by lengthening the period of growth in temperate and Mediterranean forests. Semi-arid and dry subalpine forests, however, did not benefit from an earlier onset of growth and a longer growing season, presumably due to associated water loss and/or more frequent early spring frosts. These emergent patterns of how climatic impacts on wood phenology affect tree growth at regional to hemispheric scales hint at how future phenological changes may affect the carbon sequestration capacity of extratropical forest ecosystems.

An unprecedented increase in temperature has been recorded in recent decades, with higher rates of warming outside than during the main growing season[1]. Such warming causes large changes in the timing, duration and thermal conditions of the vegetative season in extratropical terrestrial biomes[2–5]. The start of the thermal growing season (TSOS) directly influences vegetation phenology and its advance closely matches the interannual variability of spring green-up[6–12]. These phenological shifts influence the capacity of the biosphere to take up carbon[13–15] and affect the exchange of energy between the atmosphere and the biosphere[13,16]. It remains to be answered, whether the shifts in plant phenology would result in a negative feedback to warming and an increased carbon uptake or, alternatively, exhibit additional ecological stress[13]. Solving this issue may help reduce uncertainties associated with the forecasting and modelling of forest productivity and global carbon cycling.

Satellite observations of forested areas provide evidence that recent climate change has shifted foliar phenology and photosynthetic seasonality[17]. Ninety-five percent of the global land surface underwent substantial changes in foliar phenology between 1980 and 2012, including changes in the timing of phenological cycles and the vigour of vegetative activity[7]. In addition to the direct response of an advanced foliar flush to an earlier TSOS[18], peak photosynthesis occurs earlier and culminates higher in forests of the extratropical Northern Hemisphere[8,19,20]. These phenological shifts may be strongly correlated with the thermal conditions in spring because satellite data indicate that the rate of phenological change slowed under the warming hiatus of 1998–2012[21].

Changes in the timing and vigour of vegetation activity further affect when and how carbon is assimilated by terrestrial ecosystems. The spring shifts of vegetation activity may increase ecosystem productivity due to an earlier start of carbon uptake[19] and longer vegetative seasons with more vigorous photosynthetic activity[15,22]. Widespread and contrasting responses of productivity to shifts in foliar phenology, however, have been detected across northern terrestrial ecosystems. The beneficial effects of spring warmth on growing-season productivity can be offset by water stress due to higher evapotranspiration in the summer[23–25] and by increasing carbon losses due to higher respiration in the autumn[26]. A long-term study of biomass also found that alpine plants grew earlier and faster but the increase in spring productivity was offset by a reduction in autumnal productivity due to increased water stress[27]. Thus, any attempt to explain climatic influences on terrestrial carbon uptake solely on the basis of studies of shifting foliar phenology and photosynthetic seasonality remains challenging.

The carbon residence time in tree stems is much longer than in foliage, making the former a major contributor to the long-term carbon sink in forests[28]. Tree radial growth represents the annual

[1]State Key Laboratory of Tibetan Plateau Earth System, Resources and Environment (TPESRE), Institute of Tibetan Plateau Research, Chinese Academy of Sciences, Beijing, China. [2]School of Natural Resources and the Environment, University of Arizona, Tucson, AZ, USA. [3]Laboratory of Tree-Ring Research, University of Arizona, Tucson, AZ, USA. [4]Instituto Pirenaico de Ecología (IPE-CSIC), Zaragoza, Spain. [5]College of Water Sciences, Beijing Normal University, Beijing, China. [6]Sino-French Institute for Earth System Science, College of Urban and Environmental Sciences, Peking University, Beijing, China. [7]Département des Sciences Fondamentales, Université du Québec à Chicoutimi, Chicoutimi, Quebec, Canada. [8]Key Laboratory of Vegetation Restoration and Management of Degraded Ecosystems, Guangdong Provincial Key Laboratory of Applied Botany, South China Botanical Garden, Chinese Academy of Sciences, Guangzhou, China. [9]State Key Laboratory of Earth Surface Processes and Resource Ecology, Faculty of Geographical Science, Beijing Normal University, Beijing, China. [10]CREAF, Cerdanyola del Valles, Barcelona, Spain. [11]CSIC, Global Ecology Unit CREAF-CSIC-UAB, Barcelona, Spain. ✉e-mail: liangey@itpcas.ac.cn

accumulation and fixation of carbohydrates in the stem. Importantly, wood phenology, mainly in cold areas, is closely related to temperature[29]. Wood formation in conifers begins when specific critical temperatures and photoperiods are reached[30–32]. In addition to temperature, the length of the growing season determines the available period for developing functional xylem through cell maturation and lignification, especially in cold areas[31,33]. In drier ecosystems, water availability for roots, rather than rainfall per se, is another important driver of cambial reactivation[34]. Temperature and the availability and demand of water also codetermine the rate of growth[35–37]. In addition to climate, the phenology of wood formation is also associated with physiological trade-offs with bud and foliar phenology because phytohormones produced in developing buds and foliage regulate the rate of cambial division[29,38] and can lead to changes in priorities for allocating carbon within a tree.

Fundamental but still unresolved questions are thus whether and how the advance of the TSOS in spring influences annual tree growth (and biomass accumulation) across environmental gradients. We addressed these questions by investigating the influence of TSOS on tree radial growth (represented by a ring-width index, RWI) in the extratropical Northern Hemisphere and by identifying the dominant mechanisms controlling the relationship between TSOS and growth for several regions with contrasting climates (northern Asia, northern Europe, Central Europe, the Mediterranean region, the western and eastern coast of the United States and the Colorado and Tibetan Plateaus) with different forest biomes (boreal, Mediterranean, temperate, semi-arid and dry subalpine forests). We tested the hypothesis that the shift of TSOS influences tree growth by changing its timing, duration and rate according to the influence of climate on the processes of xylem formation[35,39,40]. We assumed that a shift of TSOS would lengthen the growing season by modifying growing degree days (GDD) and the availability of soil moisture (SM) and that such phenological changes could affect growth through various ecophysiological mechanisms, depending on the ambient climatic conditions.

Results

Response of tree growth to TSOS changes. Most areas in the extratropical Northern Hemisphere had trends toward an earlier TSOS between 1948 and 2016. Correlation results show that 36.5% of these areas exhibited significant advancing trends ($P<0.05$ in a two-tailed Student *t*-test) and 49.2% at least marginally significant ($P<0.1$) (Extended Data Fig. 1). Of the RWI chronologies, 11.4% had significant simple correlations with TSOS ($P<0.05$, *t*-test) and 18.0% at least marginally significant ($P<0.1$); 7.7% had significant and 13.6% at least marginally significant partial correlations (Extended Data Fig. 1). The correlations revealed distinct spatial patterns after gridding onto a 2°×2° raster (Fig. 1). The area with negative TSOS–RWI correlations was generally larger than the area with positive correlations (56% versus 33% in the simple correlation analyses and 46% versus 36% in the partial correlation analyses; see histograms in Fig. 1c,d). Negative correlations dominated at high latitudes (>60° N), central Europe, eastern and western coastal North America, indicating that the advancing TSOS could benefit tree growth in these regions. Correlations were mainly positive for the Colorado and Tibetan Plateaus, indicating that an advance in TSOS could reduce growth in these regions. Similar patterns were found for both the simple and partial correlations.

We calculated the 30-yr (1969–1998) mean growing degree days (GST) and the 30-yr mean growing-season precipitation (GSP) to compare the ambient climatic characteristics of the RWI sites with contrasting responses to changes in TSOS. GST for the RWI chronologies with significant negative TSOS correlations was distinctly lower than for RWI chronologies with positive correlations (Fig. 1e,f). Linear regression analyses of GST and GSP further indicated a higher regression coefficient for RWI chronologies with significant negative correlations than for RWI chronologies with positive correlations. These results suggest that the advance in TSOS would probably benefit tree growth in cold areas with a lower number of GST and/or a higher GSP:GST ratio.

Relationships between TSOS and RWI in climatically distinct regions. We conducted path analyses to decompose the effect of TSOS on RWI, so that the magnitude of the underlying processes responsible for the emergent correlations could be compared. TSOS–RWI relationships of each tree-ring chronology involved in path analyses for the eight selected regions (northern Asia, northern Europe, Central Europe, the Mediterranean region, the western and eastern coast of the United States, the Colorado Plateau and the Tibetan Plateau) are shown in Extended Data Fig. 2. The path diagram was reliable in all regions; the specific model fits for each region are presented in Supplementary Table 1. The path effects showed distinct responses between regions (Fig. 2). TSOS had a negative total effect on RWI (that is, higher RWI under advanced TSOS) for boreal forests in northern Asia and Europe, temperate forests in central Europe and the east coast of the United States and for forests in the Mediterranean region and along the west coast of the United States. In boreal forests, the most pronounced pathway affecting RWI is the 'growing degree days (GDD) effect' (the path effect through the 'TSOS—GDD—RWI' path), suggesting that an advance in TSOS increases tree growth mainly through the increase in GDD. TSOS also had a negative total effect on RWI in temperate and seasonally dry Mediterranean forests but the path effect was stronger through the length of the thermal growing season (GSL) than GDD, suggesting that the beneficial effect of an advanced TSOS on growth was due to the extension of the TSOS, without a clear effect of drought due to reduced SM. In contrast, TSOS for semi-arid forests on the Colorado Plateau had a strong positive total effect on RWI (lower RWI under advanced TSOS). The positive effect through GSL combined with the effect through GDD and SM, suggests that an advance in TSOS could reduce tree growth due to the longer growing season, the increase in GDD and the decrease in SM (soil drought) caused by the increased GDD. TSOS for dry subalpine forests on the Tibetan Plateau also had a positive effect on RWI, with the main path through changes to GSL, suggesting that the unfavourable situation of an advanced TSOS for growth was mainly caused by the lengthening of the growing season.

Discussion

Our study has demonstrated that spatiotemporal shifts in TSOS can significantly and variably affect tree growth in the extratropical Northern Hemisphere. This conclusion is supported by our current understanding of the physiological mechanisms that underlie wood formation. As shown by xylogenetic studies, wood formation involves sequential processes of cambial cell division, cell enlargement and cell-wall thickening[41]. The onset of wood formation is the main factor that directly or indirectly triggers all subsequent phases of xylem maturation[39]. Small changes in the period of cell division can lead to substantial increases in xylem cell production and growth[40]. The rate of increase in xylem size peaks when the cambium is dividing vigorously and most cells are undergoing the enlarging phase. These physiological processes culminate at the end of spring and slow down in late summer and autumn when the tree ring is almost fully formed[38,41,42]. Therefore, tree growth would be enhanced by an earlier onset and also by higher growth rates during the peak growing season in cold climates. Recent xylogenetic studies have also demonstrated that a longer growing season induced by its earlier start will not benefit xylem formation in trees located in drought-prone environments. Instead, warming-induced drought could limit carbon sequestration by reducing the rate of cell production[35,37]. On the basis of these physiological mechanisms,

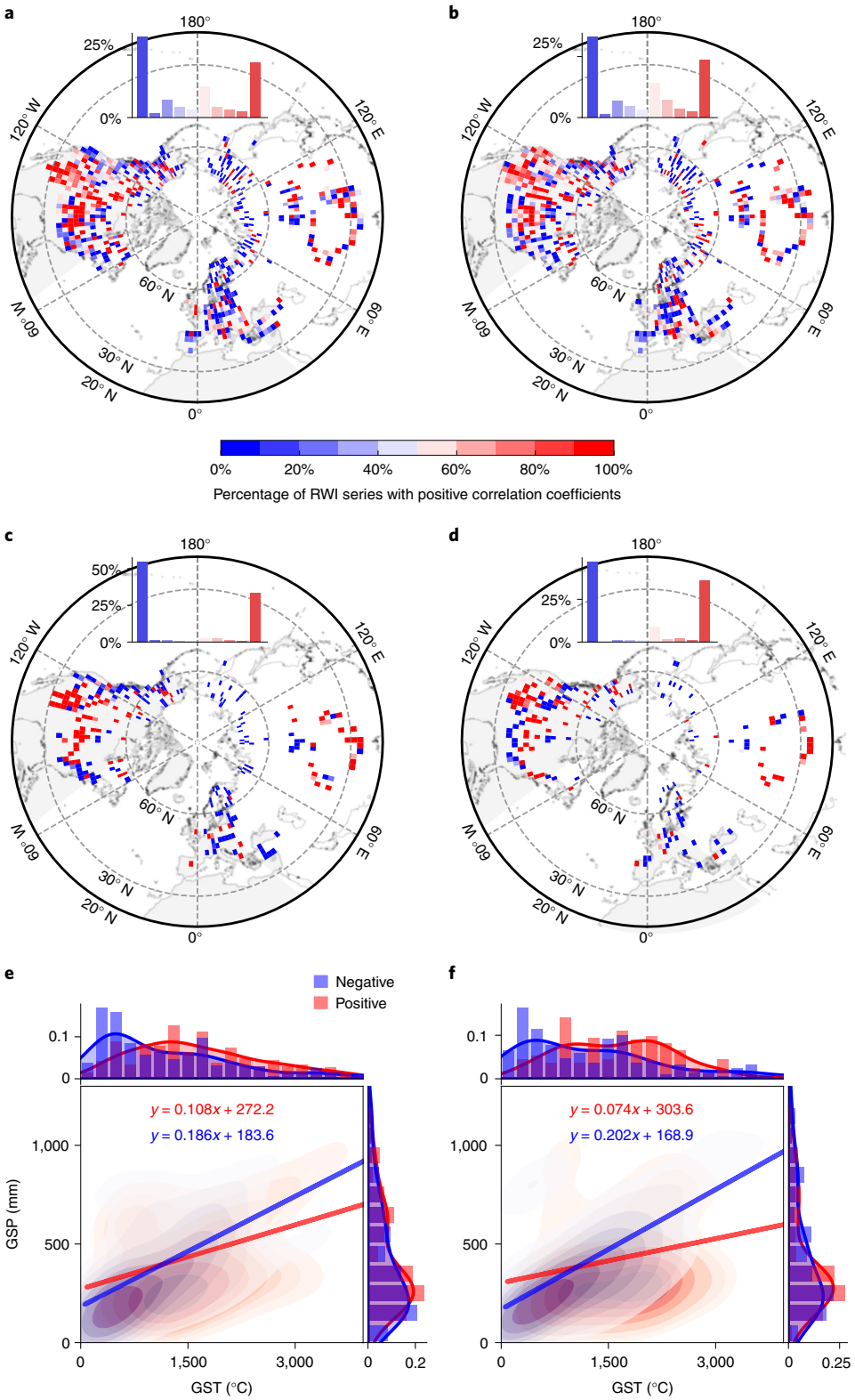

Fig. 1 | Responses of tree growth to changes in the onset of the TSOS across the extratropical Northern Hemisphere. a–d, Spatial patterns of the percentage of tree-ring series (represented by RWI) with a positive simple correlation coefficient (**a**), partial correlation coefficient (**b**), significant ($P < 0.1$) simple correlation coefficient (**c**) and significant partial correlation coefficient (**d**) between RWI and TSOS within 2° × 2° grids. The numbers of tree-ring width chronologies considered in each grid are presented in Supplementary Fig. 5. The histograms in **a–d** present the frequency distributions of the percentages. **e**,**f**, Climatic characteristics of tree-ring sites with a significant simple correlation coefficient (**e**) and partial correlation coefficient (**f**) in the space of GST and GSP. The histograms located at the top and right of **e** and **f** present the distributions of the tree-ring sites along the GST and GSP gradients. The blue and red kernel density plots and histograms represent tree-ring chronologies with negative and positive correlation coefficients, respectively. The lines in **e** and **f** are derived from linear regression, the shown regression equations are all significant ($P < 0.001$) estimated using the *F*-test.

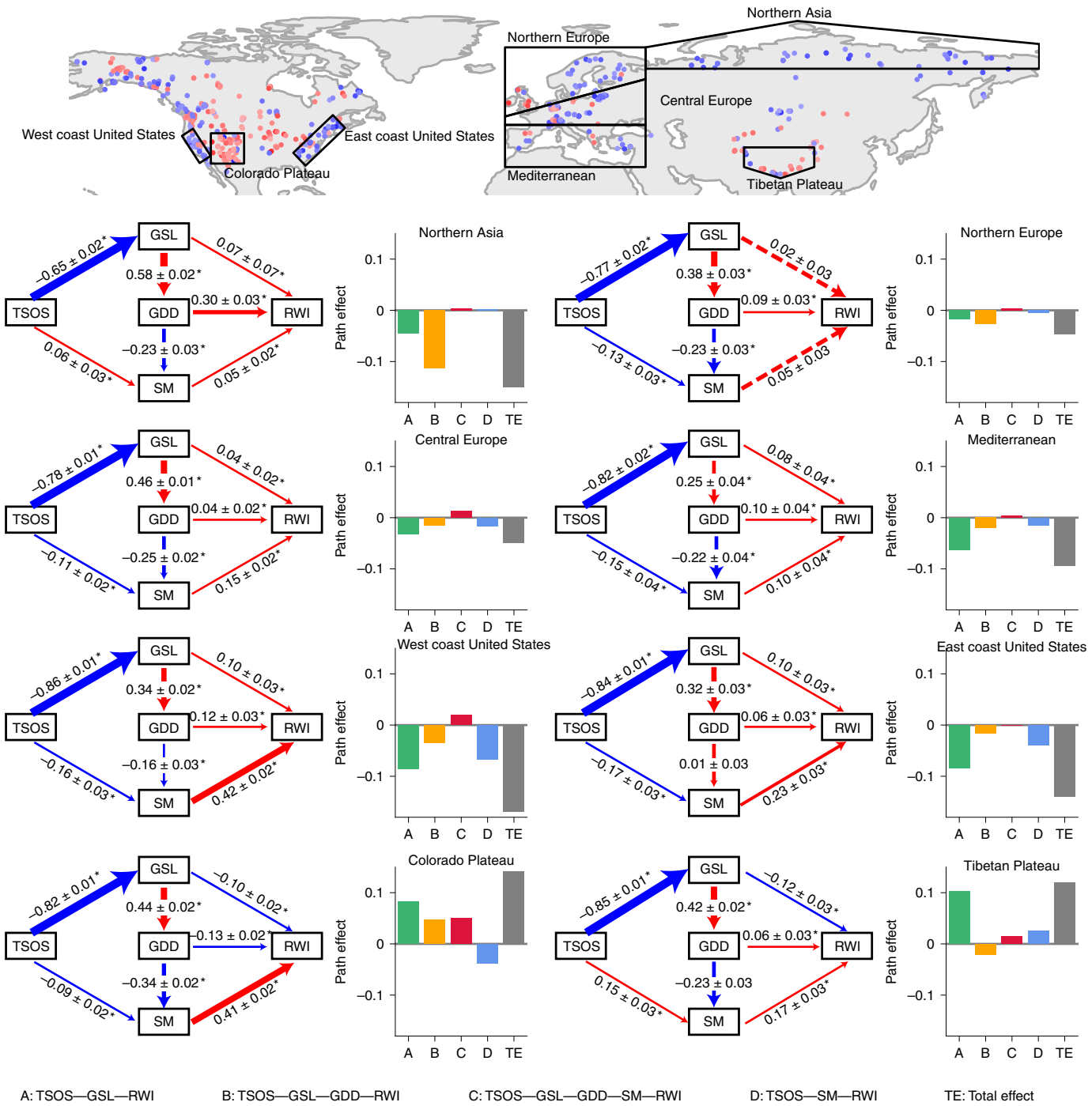

Fig. 2 | Path diagrams and path effects for northern Asia, northern and central Europe, the Mediterranean region, the west and east coasts of the United States, the Colorado Plateau and the Tibetan Plateau. In the geographic map, dots represent the location of tree-ring chronologies with significant ($P < 0.1$) positive (red dots) and negative (blue dots) simple correlation with TSOS; boxes delineate the eight regions. The numbers in the path diagrams represent the mean and standard error of standardized path coefficients in the regions, asterisks indicate the significance of the path coefficients ($P < 0.05$) and the colours (negative and positive effects are presented as blue and red arrows, respectively) and widths of the arrows represent the signs and magnitudes of the path coefficients, respectively. A, B, C and D in the panels on the right of the path diagrams represent the effect of four major paths; TE is the total effect. The number of tree-ring width chronologies for each region is presented in Supplementary Fig. 6.

we assumed that growth changes caused by shifts in TSOS can be inferred from tree-ring data.

Our results revealed a clear spatial pattern in the response of tree growth (RWI) to TSOS (Fig. 1). Areas with beneficial effects of TSOS on RWI (negative correlation) are generally located in high latitude (above 60° N), Europe, as well as in eastern and western coastal North America. These cold and humid regions have no or minimal water limitation during the growing season. This spatial distribution generally agrees with the distribution of areas that exhibit a clear advance in the timing of foliar onset and peak photosynthetic activity[11,19,43]. This importantly suggests that enhanced carbon uptake induced by the advance of TSOS promoted the

production and accumulation of photosynthates and thus increased the availability of resources for tree growth. Although a warmer autumn may offset the increased productivity during spring due to a disproportionally larger increase in respiration compared with photosynthesis[23,24,26] and can additionally cause earlier foliar senescence[44], this is likely to affect carbon stored in pools with a faster turnover rate such as shoots and leaves. However, the effect of autumnal warming was marginal for 'slow carbon' (that which is sequestered in the wood) compared to this canopy activity. The regions with negative effects of TSOS on growth (positive correlation) were mainly located on the Colorado Plateau and the Tibetan Plateau, corresponding to cold–dry conditions where forests are typically colimited by the availability of soil water and nutrients. Radial growth is more sensitive to low temperatures or drought than photosynthesis[45] and may cease long before carbon uptake in response to water shortage[46]. Warming during the growing season in these regions may intensify drought, inhibit woody tissue formation[37,45] and reverse the positive effects of temperature on growth even in cold areas[47]. An extended growing season may also increase the risk of tree exposure to low temperature events such as spring frosts[48]. These effects are possible causes of reduced tree growth and constrain carbon accumulation in the wood.

The shift in the timing of TSOS may have affected GSL, GDD and SM. The change of GSL would extend the time when cambial activity and wood formation are possible. In contrast, the change of GDD and SM would affect growth rates[35,49]. All these factors can interact to modulate tree growth and the resulting sequestration of carbon. Decomposing the effect of TSOS on radial growth in different forest biomes—as we have done in this study—can therefore help advance our understanding of the effects of TSOS on carbon sequestration and wood formation and pave the way for improved forecasting of forest carbon cycling.

The advance of TSOS benefited tree growth in the boreal forests of northern Asia and Europe and the path analyses indicated that the 'GDD effect' was the primary responsible pathway (Fig. 2a). Our results are consistent with previous studies of canopy processes reporting that an increase in vegetation greenness was more pronounced across boreal ecosystems than in other regions[50], which was mainly due to the alleviation of the limitation of cold temperatures on vegetation growth under climatic warming[51,52]. The advance of TSOS also benefited tree growth in temperate forests of central Europe and the east coast of the United States and Mediterranean forests of the Mediterranean region and the west coast of the United States. The 'GSL effect' was the primary path effect in those areas (Fig. 2b). In central Europe and along the east coast of the United States, precipitation ranges from adequate to abundant and the summers are generally warm and humid. A lengthened GSL extends the growth duration and favours tree growth there. The Mediterranean climate is characterized by dry and hot summers, with optimal conditions for vegetation growth occurring during the cool and rainy springs and autumns, often leading to a bimodal pattern of growth with a temporary cessation of growth in summer[53]. Photoperiods are longer in spring than in autumn and an earlier reactivation of the cambium after winter dormancy can harness this period for increasing production. A lengthening of the growing season through the advance of TSOS may therefore benefit tree growth if spring droughts are not persistent or severe. SM at the beginning of the growing season is also a major factor affecting tree radial growth[54,55] but the advanced TSOS in our study may have had a limited effect on RWI via the 'SM effects' (the path effect through the 'TSOS—GSL—GDD—SM—RWI' and 'TSOS—SM—RWI' paths) in these regions. The thermal conditions at the beginning of the growing season were mild and may not have caused a severe loss of soil water through evaporation but an advanced TSOS may accelerate snow melt and increase the availability of soil water[56]. These remaining uncertainties need to be comprehensively addressed in future studies. The path effects of northern and central Europe are small compared with other regions, perhaps due to the difference in the distance from the ocean and the complexity in topography and species composition, which also need to be studied with more detail in future work.

The advance of TSOS negatively affected growth in semi-arid forests on the Colorado Plateau and dry subalpine forests on the Tibetan Plateau. Path analysis further indicated that growth reductions under advanced TSOS were primarily caused by the 'GSL effect' (Fig. 2). This result was not consistent with our original hypothesis in the path diagram that an extended GSL would enhance tree radial growth (Supplementary Fig. 1) and may involve more complex mechanisms. Extended GSL in these regions, combined with higher heat accumulation ('GDD effect') and/or evapotranspiration of soil water (the path effect through the 'TSOS—GSL—GDD—SM—RWI'), may induce both atmospheric and soil droughts. Droughts will trigger stomatal closure, increase water tension in the xylem and deplete the contents of non-structural carbohydrates in trees[57–59], thus reducing the rate of wood production[35]. Forests in these regions also suffered more from frost days than those in high latitude regions (Supplementary Fig. 2). Earlier TSOS may increase tree exposure to spring frost and thereby reduce tree growth[48,60]. The specific mechanisms underlying these processes need to be addressed in further experimental studies.

Uncertainties in our analyses were mainly introduced by three sources: the spatial representativeness of the tree-ring series, the determination of the TSOS thresholds and the establishment of the path diagram. The International Tree-Ring Data Bank (ITRDB) dataset contains a large imbalance in the spatial distribution of sites and in its species composition[61,62]. Further, the local microenvironment, stand structure or biotic and abiotic disturbances are often unknown but can also impact tree radial growth and phenological responses[10,63,64]. To mitigate potential biases associated with these caveats, we first gridded the correlation coefficients and then displayed the percentage of the direction instead of the magnitude of the correlation coefficients. We were thereby able to extract the dominant spatial patterns of the response of tree growth to shifts in the timing of the TSOS.

The thermal threshold for growth of 5 °C is widely accepted and used[6] but debatable because the choice of threshold may lead to different conclusions[4]. A more vegetative-based threshold (for instance, the threshold from vegetation greenness) is, however, difficult to achieve due to the inconsistency in temporal availability of tree-ring data and satellite-retrieved observations[62]. Biological evidence suggests that the daily mean temperature threshold for the onset of xylem growth in conifers at high altitudes and in cold climates is 5.6–8.0 °C (refs. [32,65]). The critical threshold of mean air temperature at alpine treelines is ~3.9 °C (ref. [31]). With these premises, we assumed that the threshold for TSOS and GDD ranges between 4 and 6 °C while exploring the response of tree growth to TSOS at large-spatial scales and chose to present the results for the 5 °C cutoff. Reassuringly, the results of analyses with other cutoffs showed similar patterns, confirming the robustness of the results.

The establishment of our path diagram was based on experimental studies; advanced TSOS would extend growth duration (indicated by GSL) and affect growth rates (controlled by GDD and SM), thus influencing annual tree growth. Path analysis is an extension of multiple linear regression. We therefore assumed that the relationships among the variables were mainly linear, which is not always consistent with our current understanding of the complex responses of tree growth to climate[66–68]. Encouragingly, the relationships between TSOS and RWI in the eight regions were mostly linear (Extended Data Fig. 2). We therefore considered our use of path analyses to be appropriate.

We found that the impact of shifts in the timing and duration of the TSOS could be detected in tree rings at regional to

hemispheric scales. Our study thus allows for the further exploration of the impact of climatic trends and variability on tree growth. Such information is essential for integrating information regarding the responses of foliage and stems to climate change and for predicting future vegetation performance. Explaining the influence of plant phenology on carbon sequestration solely on the basis of the perspective of foliar phenology and photosynthesis seasonality (which drive carbon uptake) is insufficient. Low temperatures and drought constrain growth more than photosynthesis[45]. A carbon sink (wood) oriented view on phenological impacts is therefore essential for predicting carbon sequestration capacity because wood is the primary long-term carbon storage pool in forests. Wood formation, however, is notoriously difficult to quantify using satellite observations or techniques of eddy covariance[41]. Our study implies that the analysis of tree rings at regional to global scales could provide new solutions to differentiate between shifts in the turnover of 'slow' and 'fast' carbon pools under a rapidly changing climate[69].

In summary, our study provides strong evidence that shifts in TSOS influence tree radial growth in the extratropical Northern Hemisphere. The advance of TSOS is more likely to enhance tree growth in cold humid areas with a higher water:heat ratio, whereas growth in cold–dry areas may be reduced. Our results also indicated that the primary path effect of TSOS on growth differed among forest biomes. The beneficial effects in the boreal forests of northern Asia and Europe were mainly due to the alleviation of thermal limitation on wood formation, so that higher growth rates were possible but the primary beneficial effect in the temperate forests of central Europe and the east coast of the United States and Mediterranean forests involved a lengthening of the growing season. The negative effects for semi-arid and dry alpine forests on the cold–dry Colorado Plateau and the Tibetan Plateau were primarily due to a longer period of growth, presumably due to associated droughts driven by heat, as well as by an increased likelihood of spring frosts. This study reveals how climate affects tree growth through wood phenology and contributes to improving our ability to predict trends in the capacity of forests to sequester carbon at regional to global scales.

Methods

Experimental design. We raised fundamental but still unresolved questions of whether and how the advance of the TSOS in spring influences tree growth across environmental gradients. We addressed these questions by investigating the relationships between TSOS and tree radial growth across the extratropical Northern Hemisphere with correlation analyses and by identifying the dominant mechanisms controlling the relationships in path analyses for several regions with contrasting climates. A total of 3,451 tree-ring width chronologies and daily climatic data for 1948–2014 were used to conduct these analyses.

Data. *Tree-ring width chronologies.* Raw tree-ring width chronologies from 4,219 sites across the extratropical Northern Hemisphere (20–75° N) were selected from the reformatted dataset of ITRDB[61], as well as 83 sites on the Tibetan Plateau (Supplementary Table 2) from the tree-ring group of the Institute of Tibetan Plateau Research Chinese Academy of Sciences (ITPCAS) (https://doi.org/10.11888/Terre.tpdc.271925). We excluded chronologies <30 yr after 1948 and those where TSOS varied little (no change of TSOS for >20 yr), for a total of 3,451 sites retained for further analyses. Of these chronologies, 73.6% (2,540) were from evergreen conifers, 9.1% (314) from deciduous conifers (mainly larch), 16.5% (569) from broadleaf species and 0.2% (7) from shrubs at the boreal treeline. Twenty-one chronologies lacked information about tree species. To transform the tree-ring width data into a RWI that accentuates the variability of annual to decadal growth, we removed long-term trends caused by aging and increasing trunk diameter by fitting either a negative exponential curve or a cubic smoothing spline (removing 50% of the variance for a period of 67% of series length) to the raw ring-width series using the dplR package (v.1.7.1)[70] in R (ref. [71]). Mean site chronologies of RWI after 1948 were calculated using biweight robust means.

Climatic and SM data. Daily grids of mean air temperature and total precipitation for 1948–2016 were obtained from the Global Meteorological Forcing Dataset of the Terrestrial Hydrology Research Group at Princeton University (http://hydrology.princeton.edu/data.pgf.php) at a spatial resolution of 0.25° (ref. [72]). Daily SM content in the root zone (0–100 cm) was obtained from the NASA Global Land Data Assimilation System v.2 (GLDAS-2) (https://disc.gsfc.nasa.gov/datasets/GLDAS_CLSM025_D_2.0/summary?keywords=GLDAS2.0) at a resolution of 0.25°. GLDAS-2 is forced entirely with the Princeton meteorological forcing input data and provides a temporally consistent series from 1948 to 2014.

We extracted the timing and length of the TSOS for each year on the basis of daily mean air temperature. TSOS was defined as the first six uninterrupted days with daily mean temperatures >5 °C at mid and high latitudes[73]. The end of the thermal growing season (TEOS) was defined as the first six uninterrupted days after 1 July with daily mean temperatures <5 °C. The GSL was calculated as the time between TSOS and TEOS.

GDD, which represent the effective accumulation of heat for vegetation growth during the growing season, were calculated as the sum of daily mean temperatures >5 °C (ref. [54]):

$$\mathrm{GDD} = \sum_{\mathrm{TSOS}}^{\mathrm{TEOS}} (T_i - 5) \text{ if } T_i > 5 \quad (1)$$

where T_i is the mean temperature on day i.

GSP was calculated as the sum of daily precipitation during the thermal growing season. Mean SM during the growing season was the average of the daily content in the root zone during the thermal growing season. The 30-yr mean GDD (GST) and the 30-yr mean GSP were calculated for 1969–1998. When choosing an aridity metric for our study, we decided to use a simple index that relies only on the most widely measured variables: temperature and precipitation. We favoured the GSP:GST ratio (similar to the Selyaninov hydrothermic coefficient[74]) over more complex indices because the latter often require input variables that are best measured locally. These include atmospheric or even SM content, which are not ubiquitously available in remote areas, to feed the data pipelines that produce global gridded climate products. We thus deemed the GSP:GST ratio to be a robust, reliable and well-established aridity metric for our study. It was used to compare aridity condition during the growing season among tree-ring sites.

Analyses. *Correlations.* We calculated both simple and partial Pearson correlations to explore the effects of TSOS on tree growth for each site of tree-ring chronology. We eliminated the effects of GSL, GDD and SM when calculating partial correlation coefficients between TSOS and RWI. Tree-ring width chronologies are probably codriven by local site factors such as microclimatic and soil conditions, forest composition and competition in closed-canopy stands and a possible mismatch between the site location and the gridded climatic data (for example, elevation). To reduce the impact of these site-specific factors and identify general spatial pattern in the correlation coefficients, we gridded the correlation coefficients by 2°×2° and displayed the percentage of tree-ring series with positive coefficients within each grid.

Path analysis. Path analysis is an extension of multiple regression analyses used to evaluate causal models by examining the linear relationships between independent and dependent variables[75]. Path analysis decomposes bivariate correlation coefficients into path coefficients, which represent the relative importance of prespecified hypotheses within the same path diagram. We used the existing information of how TSOS affects RWI (introduction) to test a path diagram containing four hypothetical associations (Supplementary Fig. 1). First, the advance in TSOS would extend GSL and thereby enhance tree radial growth (represented by RWI). Second, the advance in TSOS would extend GSL and increase GDD, causing a positive change in RWI. Third, the advance in TSOS would extend GSL, increase GDD and lead to a shortage of SM, with negative effects on RWI. Fourth, the change in TSOS could affect SM by accelerating snow melt, by increasing the thawing of permafrost or by changing the proportion of precipitation during the growing season[56], thereby promoting tree growth and increasing RWI.

We used the 'sem' package (v.3.1.9)[76] in R to calculate the standardized path coefficients of the preset path diagram. Path effects were then calculated as the product of the standardized path coefficients along each pathway. We compared the bivariate correlation coefficients (TSOS and RWI) and the total path effects (the sum of the four path effects) of all 3,451 RWI series to determine the fit of the preset path diagram to our data. The relationships between the bivariate correlation coefficients and the total path effects were consistent (Supplementary Fig. 3).

We selected eight regions on the basis of the spatial patterns identified by the correlation analyses and climatological consistency to examine the general characteristics of the path effects. The definition of northern Asia and Europe, central Europe, the Mediterranean region and the Tibetan Plateau referred to IPCC climate reference regions[77], the west and east coast of the United States and the Colorado Plateau referred to the hydrologic and geographic unit. For the eight regions, general climatic conditions were presented in Supplementary Fig. 4 and forest conditions were described in the Supplementary text. Because we aimed to decompose correlations into different processes for the interpretation of underlying mechanisms, only RWI chronologies with at least marginally significant correlations ($P < 0.1$) were included in the regional path analyses[56]. Anomalies of climatic variables (TSOS, GSL, GDD and SM) were calculated for each RWI chronology in reference to its 30-yr (1969–1998) mean climate condition. Then

we used RWIs and their corresponding climatic anomalies within the same region to conduct the path analysis. All variables were standardized before path analyses. Many fitting measures can appraise a path diagram. We measured the adequacy of the fitness of the path diagram in each region using the following criteria: goodness-of-fit index ≥ 0.95, comparative fit index ≥ 0.90, root mean square error of approximation ≤ 0.10, non-normed fit index ≥ 0.92 and standardized root mean square residual ≤ 0.08. The path diagram was considered reliable when three of these five criteria were met[78].

Results validation. To confirm the robustness of our results, we tested different thresholds of TSOS, as well as of GDD at 4, 4.5, 5.5 and 6 °C and conducted the full analysis for each of them. The results showed similar pattern and are presented in Supplementary Table 3.

Reporting Summary. Further information on research design is available in the Nature Research Reporting Summary linked to this article.

Data availability

The reformatted data of the ITRDB were obtained from https://doi.org/10.5061/dryad.kh0qh06. Tree-ring width data from the ITPCAS tree-ring group are available from https://doi.org/10.11888/Terre.tpdc.271925. The Global Meteorological Forcing Dataset of the Terrestrial Hydrology Research Group at Princeton University was obtained from http://hydrology.princeton.edu/data.pgf.php. The NASA Global Land Data Assimilation System v.2 was obtained from https://disc.gsfc.nasa.gov/datasets/GLDAS_CLSM025_D_2.0/summary?keywords=GLDAS2.0. Source data are provided with this paper.

Code availability

Statistical analyses in this study were performed with publicly available packages in R (v.3.6.2, dplR and sem packages) and Python (v.3.8, scipy package) and the figures were produced using Python (matplotlib, cartopy and seaborn packages). The custom code for the analysis of the data are available from https://doi.org/10.11888/Terre.tpdc.271925.

Received: 27 July 2021; Accepted: 13 January 2022;
Published online: 28 February 2022

References

1. Trenberth, K. E. & Jones, P. D. in *Climate Change 2007: The Physical Science Basis* (eds Solomon, S. et al.) 235–335 (Cambridge Univ. Press, 2007).
2. Linderholm, H. W. Growing season changes in the last century. *Agr. For. Meteorol.* **137**, 1–14 (2006).
3. Yang, B. et al. New perspective on spring vegetation phenology and global climate change based on Tibetan Plateau tree-ring data. *Proc. Natl Acad. Sci. USA* **114**, 6966–6971 (2017).
4. Shen, M., Tang, Y., Chen, J. & Yang, W. Specification of thermal growing season in temperate China from 1960 to 2009. *Clim. Change* **114**, 783–798 (2012).
5. Zhou, B., Zhai, P., Chen, Y. & Yu, R. Projected changes of thermal growing season over Northern Eurasia in a 1.5 °C and 2 °C warming world. *Environ. Res. Lett.* **13**, 35004 (2018).
6. Barichivich, J., Briffa, K. R., Osborn, T. J., Melvin, T. M. & Caesar, J. Thermal growing season and timing of biospheric carbon uptake across the Northern Hemisphere. *Glob. Biogeochem. Cycles* **26**, B4015 (2012).
7. Buitenwerf, R., Rose, L. & Higgins, S. I. Three decades of multi-dimensional change in global leaf phenology. *Nat. Clim. Change* **5**, 364–368 (2015).
8. Gonsamo, A., Chen, J. M. & Ooi, Y. W. Peak season plant activity shift towards spring is reflected by increasing carbon uptake by extratropical ecosystems. *Glob. Change Biol.* **24**, 2117–2128 (2018).
9. Menzel, A. et al. European phenological response to climate change matches the warming pattern. *Glob. Change Biol.* **12**, 1969–1976 (2006).
10. Montgomery, R. A., Rice, K. E., Stefanski, A., Rich, R. L. & Reich, P. B. Phenological responses of temperate and boreal trees to warming depend on ambient spring temperatures, leaf habit, and geographic range. *Proc. Natl Acad. Sci. USA* **117**, 10397–10405 (2020).
11. Piao, S. et al. Leaf onset in the northern hemisphere triggered by daytime temperature. *Nat. Commun.* **6**, 6911 (2015).
12. Barichivich, J. et al. Large-scale variations in the vegetation growing season and annual cycle of atmospheric CO_2 at high northern latitudes from 1950 to 2011. *Glob. Change Biol.* **19**, 3167–3183 (2013).
13. Peñuelas, J., Rutishauser, T. & Filella, I. Phenology feedbacks on climate change. *Science* **324**, 887–888 (2009).
14. Piao, S. et al. Weakening temperature control on the interannual variations of spring carbon uptake across northern lands. *Nat. Clim. Change* **7**, 359–363 (2017).
15. Richardson, A. D. et al. Influence of spring and autumn phenological transitions on forest ecosystem productivity. *Philos. Trans. R. Soc. B* **365**, 3227–3246 (2010).
16. Bonan, G. B. Forests and climate change: forcings, feedbacks, and the climate benefits of forests. *Science* **320**, 1444–1449 (2008).
17. Piao, S. et al. Plant phenology and global climate change: current progresses and challenges. *Glob. Change Biol.* **25**, 1922–1940 (2019).
18. Fu, Y. H. et al. Declining global warming effects on the phenology of spring leaf unfolding. *Nature* **526**, 104–107 (2015).
19. Park, T. et al. Changes in timing of seasonal peak photosynthetic activity in northern ecosystems. *Glob. Change Biol.* **25**, 2382–2395 (2019).
20. Xu, C., Liu, H., Williams, A. P., Yin, Y. & Wu, X. Trends toward an earlier peak of the growing season in Northern Hemisphere mid-latitudes. *Glob. Change Biol.* **22**, 2852–2860 (2016).
21. Wang, X. et al. No trends in spring and autumn phenology during the global warming hiatus. *Nat. Commun.* **10**, 2389 (2019).
22. Piao, S., Friedlingstein, P., Ciais, P., Viovy, N. & Demarty, J. Growing season extension and its impact on terrestrial carbon cycle in the Northern Hemisphere over the past 2 decades. *Glob. Biogeochem. Cycles* **21**, B3018 (2007).
23. Buermann, W., Bikash, P. R., Jung, M., Burn, D. H. & Reichstein, M. Earlier springs decrease peak summer productivity in North American boreal forests. *Environ. Res. Lett.* **8**, 24027 (2013).
24. Buermann, W. et al. Widespread seasonal compensation effects of spring warming on northern plant productivity. *Nature* **562**, 110–114 (2018).
25. Lian, X. et al. Summer soil drying exacerbated by earlier spring greening of northern vegetation. *Sci. Adv.* **6**, eaax0255 (2020).
26. Piao, S. et al. Net carbon dioxide losses of northern ecosystems in response to autumn warming. *Nature* **451**, 49–52 (2008).
27. Wang, H. et al. Alpine grassland plants grow earlier and faster but biomass remains unchanged over 35 years of climate change. *Ecol. Lett.* **23**, 701–710 (2020).
28. Pan, Y. et al. A large and persistent carbon sink in the world's forests. *Science* **333**, 988–993 (2011).
29. Delpierre, N. et al. Temperate and boreal forest tree phenology: from organ-scale processes to terrestrial ecosystem models. *Ann. For. Sci.* **73**, 5–25 (2016).
30. Huang, J. et al. Photoperiod and temperature as dominant environmental drivers triggering secondary growth resumption in Northern Hemisphere conifers. *Proc. Natl Acad. Sci. USA* **117**, 20645–20652 (2020).
31. Li, X. et al. Critical minimum temperature limits xylogenesis and maintains treelines on the southeastern Tibetan Plateau. *Sci. Bull.* **62**, 804–812 (2017).
32. Rossi, S. et al. Critical temperatures for xylogenesis in conifers of cold climates. *Glob. Ecol. Biogeogr.* **17**, 696–707 (2008).
33. Lenz, A., Vitasse, Y., Hoch, G. & Körner, C. Growth and carbon relations of temperate deciduous tree species at their upper elevation range limit. *J. Ecol.* **102**, 1537–1548 (2014).
34. Zeng, Q., Rossi, S., Yang, B., Qin, C. & Li, G. Environmental drivers for cambial reactivation of Qilian junipers (*Juniperus przewalskii*) in a semi-arid region of northwestern China. *Atmosphere* **11**, 232 (2020).
35. Ren, P. et al. Growth rate rather than growing season length determines wood biomass in dry environments. *Agr. For. Meteorol.* **271**, 46–53 (2019).
36. Sanginés De Cárcer, P. et al. Vapor-pressure deficit and extreme climatic variables limit tree growth. *Glob. Change Biol.* **24**, 1108–1122 (2017).
37. Zhang, J. et al. Drought limits wood production of *Juniperus przewalskii* even as growing seasons lengthens in a cold and arid environment. *Catena* **196**, 104936 (2021).
38. Huang, J., Deslauriers, A. & Rossi, S. Xylem formation can be modeled statistically as a function of primary growth and cambium activity. *New Phytol.* **203**, 831–841 (2014).
39. Rossi, S., Morin, H. & Deslauriers, A. Causes and correlations in cambium phenology: towards an integrated framework of xylogenesis. *J. Exp. Bot.* **63**, 2117–2126 (2012).
40. Rossi, S., Girard, M. J. & Morin, H. Lengthening of the duration of xylogenesis engenders disproportionate increases in xylem production. *Glob. Change Biol.* **20**, 2261–2271 (2014).
41. Cuny, H. E. et al. Woody biomass production lags stem-girth increase by over one month in coniferous forests. *Nat. Plants* **1**, 15160 (2015).
42. Pasho, E., Camarero, J. J. & Vicente-Serrano, S. M. Climatic impacts and drought control of radial growth and seasonal wood formation in *Pinus halepensis*. *Trees* **26**, 1875–1886 (2012).
43. Keenan, T. F. et al. Net carbon uptake has increased through warming-induced changes in temperate forest phenology. *Nat. Clim. Change* **4**, 598–604 (2014).
44. Chen, L. et al. Leaf senescence exhibits stronger climatic responses during warm than during cold autumns. *Nat. Clim. Change* **10**, 777–780 (2020).
45. Körner, C. Paradigm shift in plant growth control. *Curr. Opin. Plant Biol.* **25**, 107–114 (2015).
46. Muller, B. et al. Water deficits uncouple growth from photosynthesis, increase C content, and modify the relationships between C and growth in sink organs. *J. Exp. Bot.* **62**, 1715–1729 (2011).
47. Charney, N. D. et al. Observed forest sensitivity to climate implies large changes in 21st century North American forest growth. *Ecol. Lett.* **19**, 1119–1128 (2016).

48. Liu, Q. et al. Extension of the growing season increases vegetation exposure to frost. *Nat. Commun.* **9**, 426 (2018).
49. Deslauriers, A. & Morin, H. Intra-annual tracheid production in balsam fir stems and the effect of meteorological variables. *Trees* **19**, 402–408 (2005).
50. Piao, S. et al. Characteristics, drivers and feedbacks of global greening. *Nat. Rev. Earth Environ.* **1**, 14–27 (2020).
51. Huang, M. et al. Air temperature optima of vegetation productivity across global biomes. *Nat. Ecol. Evol.* **3**, 772–779 (2019).
52. Keenan, T. F. & Riley, W. J. Greening of the land surface in the world's cold regions consistent with recent warming. *Nat. Clim. Change* **8**, 825–828 (2018).
53. Camarero, J. J., Olano, J. M. & Parras, A. Plastic bimodal xylogenesis in conifers from continental Mediterranean climates. *New Phytol.* **185**, 471–480 (2010).
54. Fu, Y. H. et al. Unexpected role of winter precipitation in determining heat requirement for spring vegetation green-up at northern middle and high latitudes. *Glob. Change Biol.* **20**, 3743–3755 (2014).
55. Wu, X. et al. Uneven winter snow influence on tree growth across temperate China. *Glob. Change Biol.* **25**, 144–154 (2018).
56. Wang, X. et al. Disentangling the mechanisms behind winter snow impact on vegetation activity in northern ecosystems. *Glob. Change Biol.* **24**, 1651–1662 (2018).
57. Adams, H. D. et al. Experimental drought and heat can delay phenological development and reduce foliar and shoot growth in semiarid trees. *Glob. Change Biol.* **21**, 4210–4220 (2015).
58. He, W., Liu, H., Qi, Y., Liu, F. & Zhu, X. Patterns in nonstructural carbohydrate contents at the tree organ level in response to drought duration. *Glob. Change Biol.* **26**, 3627–3638 (2020).
59. Williams, A. P. et al. Temperature as a potent driver of regional forest drought stress and tree mortality. *Nat. Clim. Change* **3**, 292–297 (2012).
60. Vitasse, Y. et al. Contrasting resistance and resilience to extreme drought and late spring frost in five major European tree species. *Glob. Change Biol.* **25**, 3781–3792 (2019).
61. Zhao, S. et al. The International Tree-Ring Data Bank (ITRDB) revisited: data availability and global ecological representativity. *J. Biogeogr.* **46**, 355–368 (2019).
62. Babst, F., Poulter, B., Bodesheim, P., Mahecha, M. D. & Frank, D. C. Improved tree-ring archives will support earth-system science. *Nat. Ecol. Evol.* **1**, 8 (2017).
63. Elmore, A. J., Guinn, S. M., Minsley, B. J. & Richardson, A. D. Landscape controls on the timing of spring, autumn, and growing season length in mid-Atlantic forests. *Glob. Change Biol.* **18**, 656–674 (2012).
64. Kannenberg, S. A. et al. Drought legacies are dependent on water table depth, wood anatomy and drought timing across the eastern US. *Ecol. Lett.* **22**, 119–127 (2018).
65. Rossi, S., Deslauriers, A., Anfodillo, T. & Carraro, V. Evidence of threshold temperatures for xylogenesis in conifers at high altitudes. *Oecologia* **152**, 1–12 (2007).
66. Gao, S. et al. Dynamic responses of tree-ring growth to multiple dimensions of drought. *Glob. Change Biol.* **24**, 5380–5390 (2018).
67. Peltier, D. M. P. & Ogle, K. Tree growth sensitivity to climate is temporally variable. *Ecol. Lett.* **23**, 1561–1572 (2020).
68. Wilmking, M. et al. Global assessment of relationships between climate and tree growth. *Glob. Change Biol.* **26**, 3212–3220 (2020).
69. Seftigen, K., Frank, D. C., Björklund, J., Babst, F. & Poulter, B. The climatic drivers of normalized difference vegetation index and tree-ring-based estimates of forest productivity are spatially coherent but temporally decoupled in Northern Hemispheric forests. *Glob. Ecol. Biogeogr.* **27**, 1352–1365 (2018).
70. Bunn, A. G. A dendrochronology program library in R (dplR). *Dendrochronologia* **26**, 115–124 (2008).
71. R Core Team. *R: A Language and Environment for Statistical Computing* (R Foundation for Statistical Computing, 2019); https://www.R-project.org/
72. Sheffield, J., Goteti, G. & Wood, E. F. Development of a 50-year high-resolution global dataset of meteorological forcings for land surface modeling. *J. Clim.* **19**, 3088–3111 (2006).
73. Frich, P. L. et al. Observed coherent changes in climatic extremes during the second half of the twentieth century. *Clim. Res.* **19**, 193–212 (2002).
74. Selyaninov, G. T. About climate agricultural estimation (in Russian). *Proc. Agric. Meteorol.* **20**, 165–177 (1928).
75. Streiner, D. L. Finding our way: an introduction to path analysis. *Can. J. Psychiatry* **50**, 115–122 (2005).
76. Fox, J., Nie, Z. & Byrnes, J. sem: Structural equation models. R package version 3.1-9 https://CRAN.R-project.org/package=sem (2017).
77. Iturbide, M. et al. An update of IPCC climate reference regions for subcontinental analysis of climate model data: definition and aggregated datasets. *Earth Syst. Sci. Data* **12**, 2959–2970 (2020).
78. Bagozzi, R. P. & Yi, Y. Specification, evaluation, and interpretation of structural equation models. *J. Acad. Mark. Sci.* **40**, 8–34 (2012).

Acknowledgements

We acknowledge all contributors to the ITRDB for providing tree-ring data. This study was supported by the Second Tibetan Plateau Scientific Expedition and Research Program (2019QZKK0301), the National Natural Science Foundation of China (41907387, 42030508 and 41988101) and the China Postdoctoral Science Foundation (2019M660813). J.P. was funded by Spanish Government projects PID2019–110521GB-I00, Fundación Ramón Areces project ELEMENTAL-CLIMATE and Catalan government project SGR2017-1005.

Author contributions

S.G. and E.L. designed the research. S.G. and R.L. performed the analysis. S.G. drafted the manuscript. E.L., F.B., J.J.C., Y.H.F., S.P., S.R., M.S., T.W. and J.P. contributed ideas, interpreted the results and were involved in the editing and writing of the manuscript.

Competing interests

The authors declare no competing interests.

Additional information

Extended data is available for this paper at https://doi.org/10.1038/s41559-022-01668-4.

Supplementary information The online version contains supplementary material available at https://doi.org/10.1038/s41559-022-01668-4.

Correspondence and requests for materials should be addressed to Eryuan Liang.

Peer review information *Nature Ecology & Evolution* thanks Bao Yang, Yingying Xie and the other, anonymous, reviewer(s) for their contribution to the peer review of this work.

Reprints and permissions information is available at www.nature.com/reprints.

Publisher's note Springer Nature remains neutral with regard to jurisdictional claims in published maps and institutional affiliations.

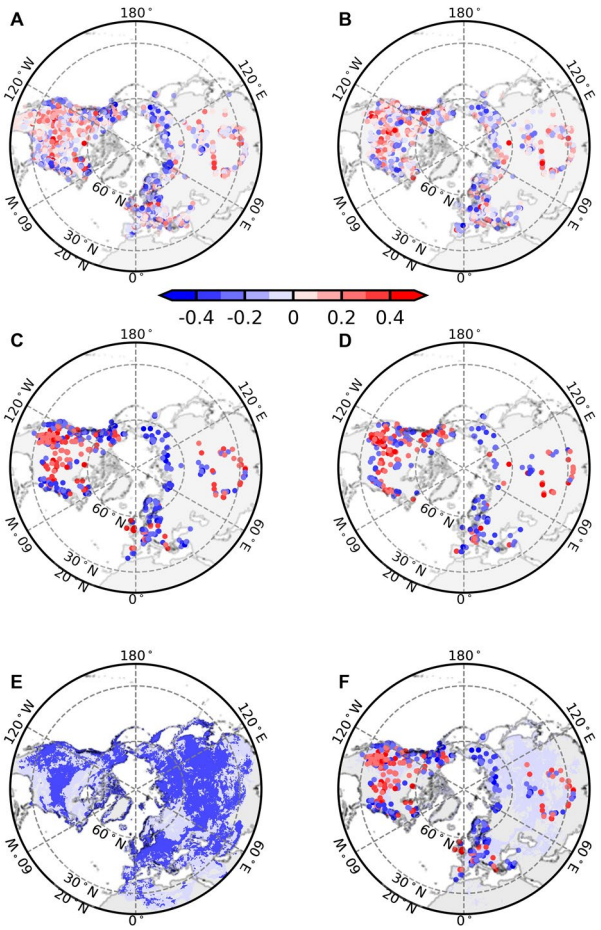

Extended Data Fig. 1 | Responses of tree growth to changes in TSOS in the extratropical Northern Hemisphere. Spatial distributions of simple correlation coefficients (A), partial correlation coefficients (B), significant ($p < 0.1$) simple correlation coefficients (C) and significant ($p < 0.1$) partial correlation coefficients (D) of TSOS and RWI. (E) Areas with significant ($p < 0.1$, dark blue) and nonsignificant (light blue) trends toward earlier TSOS between 1948 and 2016 in the extratropical Northern Hemisphere. (F) Areas with significant ($p < 0.05$, blue shaded area) trends toward earlier TSOS overlapping tree-ring chronologies with significant ($p < 0.1$) simple correlation coefficients of TSOS and RWI. The significance of the correlation analyses is estimated by two-tailed Student's *t*-test. This figure was generated using the matplotlib and cartopy package in Python.

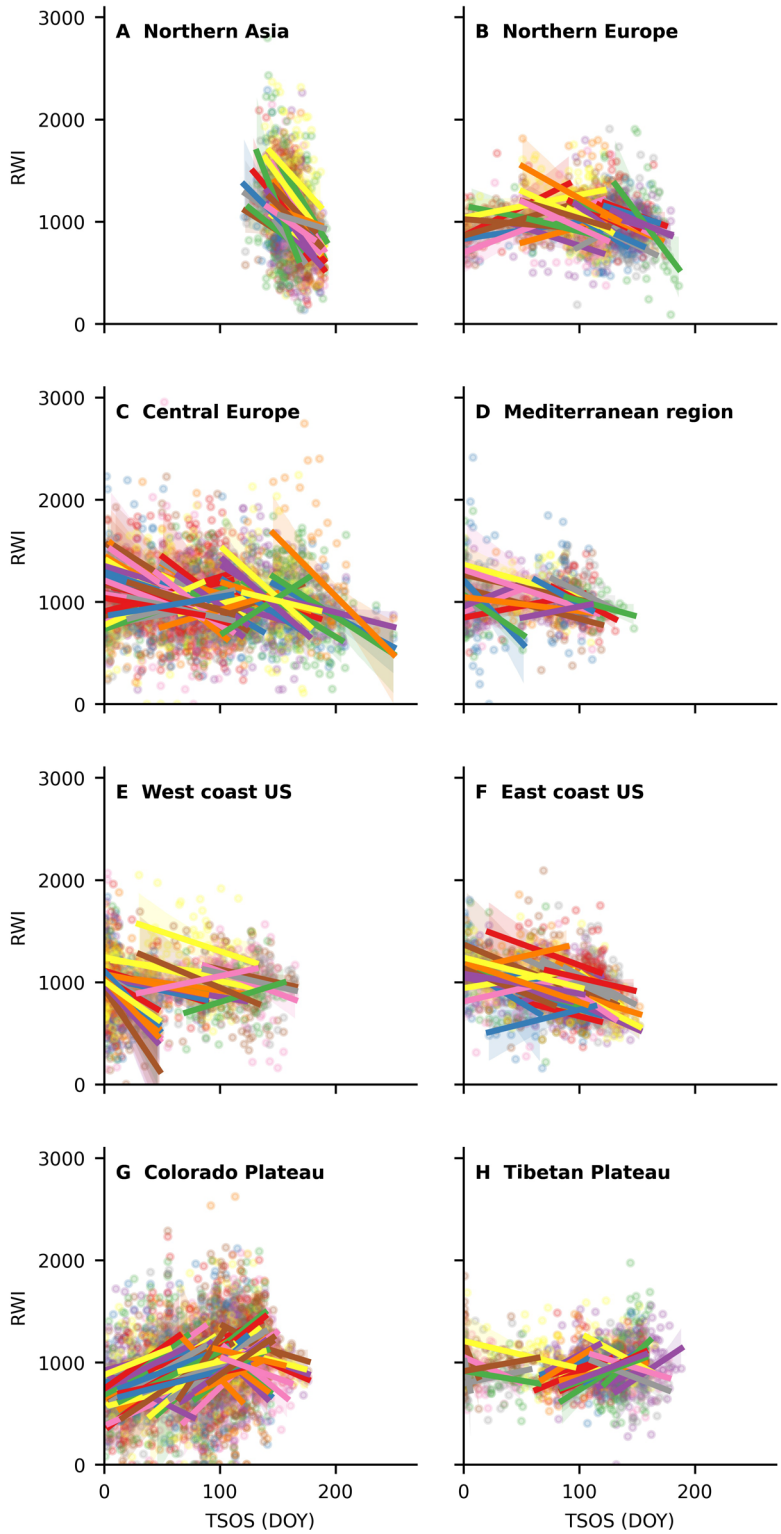

Extended Data Fig. 2 | Scatter plots of TSOS–RWI relationships in different regions. TSOS–RWI relationships of tree-ring chronologies with significant ($p < 0.1$) simple correlations for northern Asia (A), northern Europe (B), central Europe (C), the Mediterranean region (D), the west coast of the US (E), the east coast of the US (F), the Colorado Plateau (G) and the Tibetan Plateau (H). The predicted mean (solid lines) is bounded by the 95% confidence intervals (shaded areas). This figure was generated using the seaborn package, 'lmplot' function in Python.

nature portfolio

Corresponding author(s): Eryuan Liang

Last updated by author(s): Dec 31, 2021

Reporting Summary

Nature Portfolio wishes to improve the reproducibility of the work that we publish. This form provides structure for consistency and transparency in reporting. For further information on Nature Portfolio policies, see our Editorial Policies and the Editorial Policy Checklist.

Statistics

For all statistical analyses, confirm that the following items are present in the figure legend, table legend, main text, or Methods section.

n/a	Confirmed
☐	☒ The exact sample size (*n*) for each experimental group/condition, given as a discrete number and unit of measurement
☒	☐ A statement on whether measurements were taken from distinct samples or whether the same sample was measured repeatedly
☐	☒ The statistical test(s) used AND whether they are one- or two-sided *Only common tests should be described solely by name; describe more complex techniques in the Methods section.*
☐	☒ A description of all covariates tested
☐	☒ A description of any assumptions or corrections, such as tests of normality and adjustment for multiple comparisons
☐	☒ A full description of the statistical parameters including central tendency (e.g. means) or other basic estimates (e.g. regression coefficient) AND variation (e.g. standard deviation) or associated estimates of uncertainty (e.g. confidence intervals)
☐	☒ For null hypothesis testing, the test statistic (e.g. *F*, *t*, *r*) with confidence intervals, effect sizes, degrees of freedom and *P* value noted *Give P values as exact values whenever suitable.*
☒	☐ For Bayesian analysis, information on the choice of priors and Markov chain Monte Carlo settings
☐	☒ For hierarchical and complex designs, identification of the appropriate level for tests and full reporting of outcomes
☐	☒ Estimates of effect sizes (e.g. Cohen's *d*, Pearson's *r*), indicating how they were calculated

Our web collection on statistics for biologists contains articles on many of the points above.

Software and code

Policy information about availability of computer code

Data collection	No software was used to collect data.
Data analysis	Statistical analysis in this study were performed in R (version 3.6.2, dplR and sem packages) and python (version 3.8, scipy package), and the figures were produced using Python (matplotlib, cartopy and seaborn packages). The custom code for the analysis of the data are available from https://doi.org/10.11888/Terre.tpdc.271925

For manuscripts utilizing custom algorithms or software that are central to the research but not yet described in published literature, software must be made available to editors and reviewers. We strongly encourage code deposition in a community repository (e.g. GitHub). See the Nature Portfolio guidelines for submitting code & software for further information.

Data

Policy information about availability of data

All manuscripts must include a data availability statement. This statement should provide the following information, where applicable:

- Accession codes, unique identifiers, or web links for publicly available datasets
- A description of any restrictions on data availability
- For clinical datasets or third party data, please ensure that the statement adheres to our policy

The reformatted data set of the International Tree-Ring Data Bank were obtained from https://doi.org/10.5061/dryad.kh0qh06. Tree-ring width data from the ITPCAS tree-ring group are available from https://doi.org/10.11888/Terre.tpdc.271925. The Global Meteorological Forcing Dataset of the Terrestrial Hydrology Research Group at Princeton University were obtained from http://hydrology.princeton.edu/data.pgf.php. The NASA Global Land Data Assimilation System Version 2 were obtained from https://disc.gsfc.nasa.gov/datasets/GLDAS_CLSM025_D_2.0/summary?keywords=GLDAS2.0.

Field-specific reporting

Please select the one below that is the best fit for your research. If you are not sure, read the appropriate sections before making your selection.

☐ Life sciences ☐ Behavioural & social sciences ☒ Ecological, evolutionary & environmental sciences

For a reference copy of the document with all sections, see nature.com/documents/nr-reporting-summary-flat.pdf

Ecological, evolutionary & environmental sciences study design

All studies must disclose on these points even when the disclosure is negative.

Study description	We raised fundamental but still unresolved questions of whether and how the advance of the thermal growing season in spring influences tree growth across environmental gradients. We addressed these questions by investigating the relationships between the start of the thermal growing season (TSOS) and tree radial growth across the extratropical Northern Hemisphere with correlation analyses and by identifying the dominant mechanisms controlling the relationships in path analyses for several regions with contrasting climates. A total of 3451 tree-ring width chronologies and daily climatic data for 1948-2014 were used to conduct these analyses.
Research sample	Most of tree-ring width chronologies were from existing dataset (the reformatted data set of the International Tree-Ring Data Bank). The sampling and processing procedure of tree-ring width data from the ITPCAS tree-ring group followed the basic principles of dendrochronology.
Sampling strategy	The sampling of tree-ring width data from the ITPCAS tree-ring group followed the principles of replication in dendrochronology. Each stand-level chronology was developed from multiple tree-level series (two cores from one tree, approximately 20 trees).
Data collection	Existing datasets are downloaded from the sources. All datasets include: tree-ring width data from https://doi.org/10.5061/dryad.kh0qh06 and https://doi.org/10.11888/Terre.tpdc.271925; Daily grids of mean air temperature and total precipitation for 1948 to 2016 from http://hydrology.princeton.edu/data.pgf.php; Daily soil-moisture content from https://disc.gsfc.nasa.gov/datasets/GLDAS_CLSM025_D_2.0/summary?keywords=GLDAS2.0
Timing and spatial scale	We used tree-ring data and climate data of the extratropical Northern Hemisphere spanning from 1948 to 2014.
Data exclusions	We excluded chronologies shorter than 30 years after 1948 and those where TSOS varied little (i.e. no change of TSOS for >20 years), for a total of 3451 sites retained for further analyses.
Reproducibility	All attempts to repeat the analysis with these data and statistical methods were successful.
Randomization	Not relevant to this study. Tree-ring data are observational data under natural conditions not from manipulative experiments.
Blinding	Not relevant to this study. Investigators who have contributed tree-ring data followed the basic principles of site selection and replication.

Did the study involve field work? ☐ Yes ☒ No

Reporting for specific materials, systems and methods

We require information from authors about some types of materials, experimental systems and methods used in many studies. Here, indicate whether each material, system or method listed is relevant to your study. If you are not sure if a list item applies to your research, read the appropriate section before selecting a response.

Materials & experimental systems

n/a	Involved in the study
☒	☐ Antibodies
☒	☐ Eukaryotic cell lines
☒	☐ Palaeontology and archaeology
☒	☐ Animals and other organisms
☒	☐ Human research participants
☒	☐ Clinical data
☒	☐ Dual use research of concern

Methods

n/a	Involved in the study
☒	☐ ChIP-seq
☒	☐ Flow cytometry
☒	☐ MRI-based neuroimaging